IFSCC 2025 full paper (IFSCC2025-154)

Kopexil and Kopyrrol Co-Delivery Nanoliposomes Targeting Different Hair Regeneration Pathways for Safe and Effective Androgenetic Alopecia Treatment

Siyuan Chen[*1, 2], Jia Luo[1], Dan Chen[1], Yutong Wu[1], Jun Deng[2], Wei Liu[*2]

[1] Hangzhou Rebtech/Wuhan Best-Carrier Nanomedicine Research Institute, China;

[2] National Engineering Research Center for Nanomedicine, Huazhong University of Science and Technology, Wuhan, China

Email: maggie@hzrebtech.com, siyuan.chen@njtech.edu.cn

Abstract

Effective and safe treatment of androgenetic alopecia (AGA), the most common type of hair loss worldwide, remains a long-standing challenge. Although minoxidil remains the primary drug for AGA treatment, due to notable side effects, its application was limited. Moreover, it requires frequent use over a long time in order to be effective, leading to low patient compliance.

To address the abovementioned issues, one promising strategy is exploring alternative active ingredients targeting different hair regeneration pathways. Furthermore, an effective co-delivery platform is needed to enhance the efficacy at a lower dosage to minimize unwanted side effects. Kopexil and kopyrrol are both commercialized minoxidil derivatives with less toxicity. Kopexil stimulates HFs by enhancing vasodilation and also can prevent perifollicular fibrosis, kopyrrol could accelerate hair regrowth by optimizing the hair growth cycle and promoting the proliferation of human dermal papilla cells (HDPCs). Unfortunately their effectiveness was inferior compared to minoxidil, and the application was further hampered by low hair follicle accumulation and bioavailability. Herein, we developed a co-delivery liposomal delivery platform by co-encapsulating kopexil and kopyrrol into nanoliposomes (KK-NLPs) to effectively and safely treat AGA.

Facilitated by nanoliposomes with small particle size and high affinity with the cell membrane, the KK-NLPs considerably enhanced cellular uptake, skin retention and permeation. Notably, hair follicle accumulation and enhanced cellular internalization into HDPCs were achieved by the KK-NLPs. Moreover, the co-delivered kopexil and kopyrrol exhibited synergistic effects by coordinating an upregulation in the expression of EK, bFGF, β-catenin and vascular endothelial growth factor, and thus collectively fostering cell proliferation and migration. A pronounced antioxidative effect was achieved, with effective protection of HDPCs from oxidative damage and remarkably reduced cellular ROS level. Furthermore, KK-NLPs could reduce the cellular damage caused by testosterone and promote collagen secretion. All these unique features of KK-NLPs contribute to expediting the progression of hair follicles into the anagen phase and promoting peripheral angiogenesis, with identical or superior hair regeneration effects at a much lower dosage than minoxidil. These results suggest the great potential of this kopexil and kopyrrol co-delivery NLPs for safe and efficient AGA treatment.

---

1. Introduction

Androgenetic alopecia (AGA), the most prevalent form of hair loss, significantly compromises both quality of life and psychological well-being[1]. This condition manifests through hair thinning, follicular miniaturization, and excessive shedding. Its pathogenesis is principally driven by androgen metabolism: Type II 5α-reductase converts testosterone to the more potent dihydrotestosterone (DHT), which binds to androgen receptors (AR) and translocates to the nucleus[2]. The AR-DHT complex subsequently interacts with androgen response elements

on DNA, recruiting transcriptional co-regulators to activate target gene expression[3]. This cascade disrupts the hair growth cycle, precipitating progressive miniaturization and eventual hair loss. Contributory factors such as vascular insufficiency and oxidative stress within the follicular microenvironment further accelerate follicular atrophy.

Current FDA-approved therapy involves topical minoxidil, though its precise mechanism remains incompletely understood despite proposed roles in vasodilation and Wnt/β-catenin pathway activation[4]. Notably, adverse effects range from dermatitis and allergic reactions to potential systemic complications including hypotension and tachycardia. These limitations underscore the urgent need for safer, more effective AGA interventions[5]. One therapeutic strategy focuses on identifying alternative actives with improved safety profiles. Structurally analogous to minoxidil, both kopexil and kopyrrol demonstrate hair growth-promoting efficacy. Kopexil enhances vasodilation while mitigating perifollicular fibrosis, exhibiting fewer adverse effects than minoxidil. Despite the commercialization of kopexil and kopyrrol-containing haircare products leveraging their efficacy and reduced toxicity, no studies to date have explored their synergistic application through distinct regenerative mechanisms.

Improving the transdermal delivery efficiency of functional ingredients could also enhance the effectiveness of AGA treatment[6]. The stratum corneum (SC) constitutes a primary barrier limiting drug penetration and target-site accumulation. Emerging techniques to enhance permeation include electroporation, chemical enhancers, and nanocarriers. Nanoliposomes (NLPs), featuring a bilayer structure, offer benefits such as improved drug solubility, stability, and therapeutic index[7,8]. Their structural resemblance to SC components and follicular affinity enhance cutaneous penetration and localized drug deposition. Furthermore, NLPs' biomimetic membrane-like architecture may facilitate cellular uptake, positioning them as promising vehicles for topical AGA therapies.

In this study, we reported a NLPs codelivery of kopexil and kopyrrol to effectively promote hair regeneration. Since kopexil and kopyrrol promote hair growth with different mechanisms and are less toxic than minoxidil, codelivery of kopexil and kopyrrol via NLPs could synergistically prolong the anagen phase of the hair growth cycle, while NLPs encapsulation could improve the solubility of the active ingredients and facilitate their cellular uptake by target cells. The kopexil and kopyrrol co-loaded NLPs enhanced the transdermal permeation and AGA therapeutic efficacy. Within the target cells, the kopexil and kopyrrol released from NLPs well maintained their therapeutic effectiveness by synergistically stimulating the secretion of related factors to activate HFs and prolong the anagen phase of the hair growth cycle, suggesting its potential for effective AGA treatment.

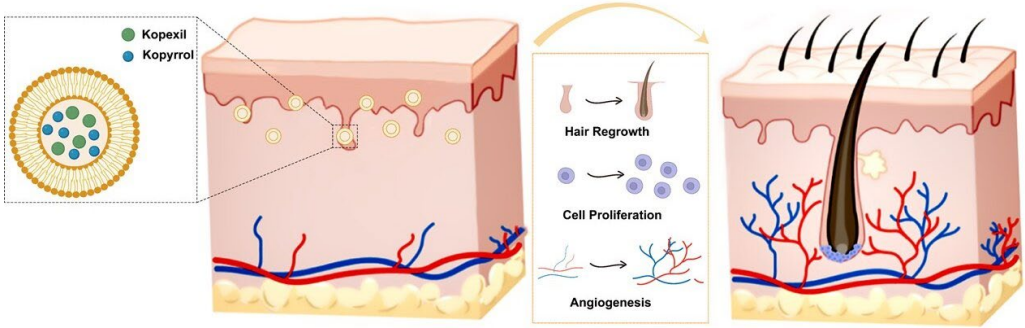

Figure 1. Schematic of kopexil and kopyrrol co-delivery nanoliposomes for safe and effective androgenetic alopecia treatment.

2. Materials and Methods

2.1 Materials

Kopexil and kopyrrol were purchased from Kumar (India). Phosphatidylcholine from soybean was obtained from Shanghai Taiwei Pharmaceutical Co., Ltd. (Shanghai, China). Cholesterol, ethanol, 1,2-propanediol, glycerol, and testosterone were obtained from Sinopharm Chemical Reagent Co., Ltd. (Shanghai, China). 4′,6-Diamidine-2′-phenylindole dihydrochloride (DAPI), rhodamine B isothiocyanate (RhoB), and minoxidil

were purchased from Aladdin (Shanghai, China). Dulbecco's modified Eagle's medium (DMEM), fetal bovine serum (FBS), phosphate-buffered saline (PBS, pH 7.4), penicillin, streptomycin, and trypsin-EDTA were obtained from Gibco (Gaithersburg, MD). Hydrogen peroxide (H_2O_2), testosterone were purchased from Sigma-Aldrich Co. (St. Louis, MO). The Cell Counting Kit-8 (CCK-8) Assay Kit was obtained from Dojindo (Kumamoto, Japan). High-performance liquid chromatography (HPLC)-grade acetonitrile was purchased from TEDIA (OH).

2.2. Cell culture

Immortalized human keratinocytes (HaCaT; American Type Culture Collection, VA, USA) were cultured in DMEM with 10% FBS and 1% penicillin/streptomycin. Human dermal papilla cells (HDPCs; SynthBio, Hefei, China) were cultured in DMEM with 20% FBS and 1% penicillin/ streptomycin. The cells were incubated in a humidified atmosphere of 5% CO_2 at 37°C.

2.3. Preparation of KK-NLPs

KK-NLPs were prepared using a high-pressure homogenization method. Briefly, 50% (*w/w*) 1,2-propanediol containing 3% (*w/w*) phosphatidylcholine from soybean, 0.2% (*w/w*) cholesterol, 5% (*w/w*) ethanol, 5% kopexil, and 2.5% kopyrrol (the ratio of kopexil to kopyrrol was fixed at 2:1) were mixed to produce phase A. Distilled water containing 10% (w/w) glycerol (phase B) was added to phase A and stirred at 65°C for 30 min, followed by homogenization at 800 bar three times to obtain KK-NLPs. Blank NLPs without drug loading or RhoB-loaded NLPs (RhoB-NLPs) were prepared using the same protocol.

2.4. Characterization of KK-NLPs.

KK-NLPs were characterized in terms of the particle size, polydispersity index (PDI), and ζ-potential by dynamic light scattering (DLS) using a Zetasizer/Nano-ZS90 instrument (Malvern Instruments, Malvern, U.K.). After being stained with 1% phosphotungstic acid, the morphology of the KK-NLPs was observed by transmission electron microscopy (TEM, HT7700, Hitachi, Tokyo, Japan). To measure the drug loading (DL) and encapsulation efficiency (EE), unloaded drugs were separated from KK-NLPs using an ultrafiltration method.

2.5. In vitro release study

To investigate the in vitro release of kopexil and kopyrrol, 1 mL of free KK (kopexil concentration of 5 mg/mL), 1 mL of KK-NLPs (with equivalent kopexil and kopyrrol concentrations as the free KK group) were enclosed within a dialysis bag (MWCO 14 kDa), then immersed in 80 mL of PBS containing 20% (w/w) 1,2-propanediol, serving as the release medium. In vitro release study was carried out in a shaker (120 rpm, 32°C). At specific time intervals (0.25, 0.5, 1, 2, 4, 6, 8, 10, and 12 h), 1 mL of the samples were withdrawn and replenished with an equal volume of fresh release medium. Subsequently, the concentration of active ingredients in the samples was determined using HPLC.

2.6. In vivo skin permeation

In vitro permeability was investigated using the Franz diffusion cell method. The porcine skin was clamped between the donor chamber and the receptor chamber, and 0.5 mL of RhoB-loaded NLPs (RhoB-NLPs) or RhoB solution (Free RhoB) was topically applied to the skin surface. 7 mL of reception medium (saline containing 20% (w/w) of 1,2-propanediol) was added to the receptor chamber, and in vitro skin permeation study was performed at 32°C with a magnetic stirring speed at 300 rpm. At specific time points (2 and 4 h) postadministration, the corresponding porcine skin of each group was harvested and the surface was washed with saline. The treated skin was subsequently embedded in the optimal cutting temperature (OCT) compound and sliced into 10-μm-thick sections using a cyrotome (CryoStar NX50, Thermo Scientific, Shanghai, China). The transdermal delivery of RhoB was visualized through a confocal laser scanning microscope (CLSM, FV3000, Olympus, Tokyo, Japan).

2.7. Cellular uptake study

HDPCs were treated with a Free KK or RhoB-NLPs at the same concentration and incubated on 35 mm glass bottom dishes for 4 h, respectively. Subsequently, the cells were washed three times with cold PBS, treated with DAPI solution to label the nucleus, and imaged with CLSM for cellular uptake.

Quantitative analysis of cellular uptake in the HDPCs was performed with flow cytometry. HDPCs were seeded in 6-well plates and incubated for 24 h. The cells were treated with RhoB-NLPs at 37°C for 2 h or 4 h. After incubation, the medium was removed and the treated cells were washed with cold PBS, trypsinized, centrifuged and resuspended in cold PBS prior to flow cytometry analysis (FC500, Beckman Coulter, Fullerton, CA, USA).

2.8. Cell migration assay

HDPCs were seeded in 6-well plates (Corning, USA) and grown to 90% confluence in 20% FBS DMEM medium. Straight lines were scratched on the cells in each well using 200 μL sterile pipette tips, followed by washing the cells three times with sterile PBS to remove cell debris. Next, the HDPCs were treated with Free KK or KK-NLPs in serum-free DMEM at a kopexi concentration of 200 μM. Photographs of the wounded area were taken under the microscope (MshOt, MF52-N, Guangzhou, China) at 0 h and 24 h.

2.9. HDPCs Proliferation Assay

The effect of KK-NLPs on the proliferation of HDPCs was determined with EdU assay. Free KK-treated, Blank NLPs-treated, KK-NLPs-treated and control-treated cells (2×10^5/dish) were seeded in 35 mm dishes (Corning, USA) for 48 h. The EdU assay was performed using the BeyoClickTM EdU Cell Proliferation Kit (Beyotime, Shanghai, China). Cells were treated according to the manufacturer's instructions and all cell nuclei were stained with DAPI. The cells were examined under a CLSM.

2.10. Testosterone-induced damage in HDPCs

HDPCs were seeded in 96-well plates and cultured for 24 h. Next, the cells were treated with Free KK or KK-NLPs in 0.1 mM testosterone at a kopexil concentration of 50, 100 or 200 μM for 24 h. Cells was treated with Blank NLPs with a lipid concentration equal to that of the KK- NLPs. HDPCs were treated with only DMEM as the control group and with only 0.1 mM testosterone for 24h as the model group. After 24-h incubation, cell viability was measured with the CCK-8 kit.

2.11. H_2O_2-induced oxidative damage in HDPCs

HDPCs were seeded in 96-well plates and cultured for 24 h. Next, the cells were treated with Free KK or KK-NLPs in 1 mM H_2O_2 at a kopexil concentration of 50, 100 or 200 μM for 24 h. Cells was treated with Blank NLPs with a lipid concentration equal to that of the KK-NLPs. HDPCs were treated with only DMEM as the control group and with only 1 mM H_2O_2 for 24h as the model group. After 24-h incubation, cell viability was measured with the CCK-8 kit.

2.12. VEGF, bFGF and Collagen III synthesis measurement

HDPCs were seeded in 96-well plates (Corning, USA) and cultured for 24 h at 37℃. Next, the cells were treated with Free KK or KK-NLPs at kopexil concentrations of 50, 100 and 200 μM. After incubation for 48 h, the content of VEGF and bFGF in the medium was determined using the VEGF Assay Kit (Beyotime, Shanghai, China) and bFGF Assay Kit (Beyotime, Shanghai, China), respectively.Human Collagen type III Assay Kit (Jiangsu Meimian Industrial Co., Ltd, Yancheng, China)

2.13. Human epidermal keratins (EK)synthesis measurement

HaCaT was seeded in 24-well plates (Corning, USA) and cultured for 24 hat 37 ◦ C. Next, the cells were treated with Free KK or KK-NLPs at kopexil concentrations of 50, 100 and 200 μM. After incubation for 48 h, the content of human epidermal keratins in the medium was determined using Human EK ELISA Kit (Jianglaibio, Shanghai, China).

2.14 RNA extraction and gene relative expression analysis

For cell culture, as shown in 2.13, the number of cells was adjusted to 1.5×10^5 /mL, 2 mL cell suspension was added to each hole of the 6-well culture plate, and the cell incubator was kept overnight. In the sample group, Free KK or KK-NLPs at kopexil concentrations of 200 μM were added, 0.1 μmol/L minoxidil was used as the positive control. After incubation for 24 h, cells were collected, total RNA was extracted by RNA extraction kit, RNA concentration and purity were analyzed by enzyme marker, and complementary DNA synthesis reaction was performed by M-MLV reverse transcriptase kit. According to the one-step fluorescence quantitative RT-PCR MasterMix kit procedure, a real-time fluorescence quantitative PCR instrument was used to perform fluorescence quantitative analysis, and the relative expression levels of the mRNA of the relevant genes were analyzed by the $2^{-\Delta\Delta Ct}$ calculation method, and the primer sequences are shown in Table 1.

Table 1 Primer sequence

Primer	Sequence（5’ -3’）
GAPDH	F: TCCATGACAACTTTGGTATC
	R: TGTAGCCAAATTCGTTGTCA
β-catenin	F: AAAGCGGCTGTTAGTCACTGG
	R: CGAGTCATTGCATACTGTCCAT
Cyclin D	F: CGTGGCCTCTAAGATGAAGG
	R: TGCGGATGATCTGTTTGTTC

2.15 Statistical analysis

All data points were replicated three times (n = 3). Results and graphical data are reported as means with 95% confidence intervals for standard deviations. Statistical significance of differences was assessed using Student ’s t-test. $p < 0.05$ was considered a statistically significant difference.

3 Results

3.1 Particle size, ζ-potential and morphology of KK-NLPs

The prepared KK-NLPs suspension displayed a transparent, pale yellow color, with a particle size of 200.3 ± 0.7 nm, a narrow size distribution (PDI of 0.109 ± 0.007), and a ζ-potential of −31.4 ± 1.0 mV (Figure 2a). As indicated in the TEM image (Figure 2b), the KK-NLPs were spherical with a distinct bilayer structure, and the particle size was consistent with the DLS data. Kopexil and kopyrrol were successfully coloaded into NLPs. The DL values of kopexil and kopyrrol in KK-NLPs were 6.56 ± 0.11 and 3.47 ± 0.05%, respectively, while the corresponding EE values were 97.2 ± 1.4 and 98.3 ± 1.5%.

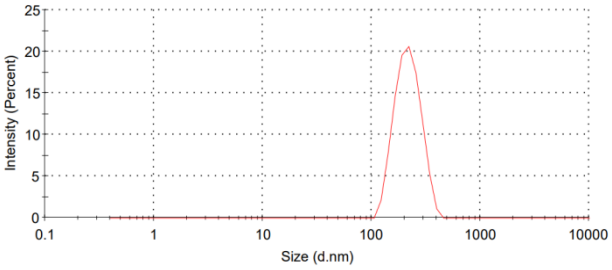

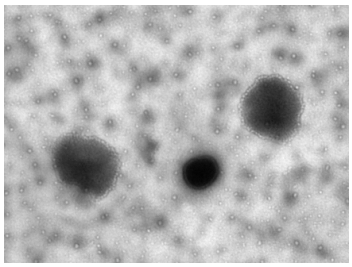

(**a**) (**b**)

Figure 2. Characterization of KK-NLPs. (a) Particle size distribution. (b) TEM image.

3.2 In vitro drug release

The release profiles of kopexil and kopyrrol encapsulated in NLPs and free peptides are shown in Figure 3a and 3b. Free KK showed faster release, and the cumulative released amounts of kopexil (91.1%) and kopyrrol (95.6%) were significantly higher than their cumulative level released from KK-NLPs within 48 h, as followed 62.8% and 72.4% respectively.

3.3 Safety Evaluation

The cellular safety evaluation results of different concentrations of Free KK and KK-NLPs on HaCaT cells and HDPC cells are shown in Figure 4a and 4b. Within the kopexil

concentration range of 0.5 to 8 mM, both the Free KK and the KK-NLPs exhibit over 90 % cell viability for HaCaT and HDPC cells, indicating no cytotoxicity.

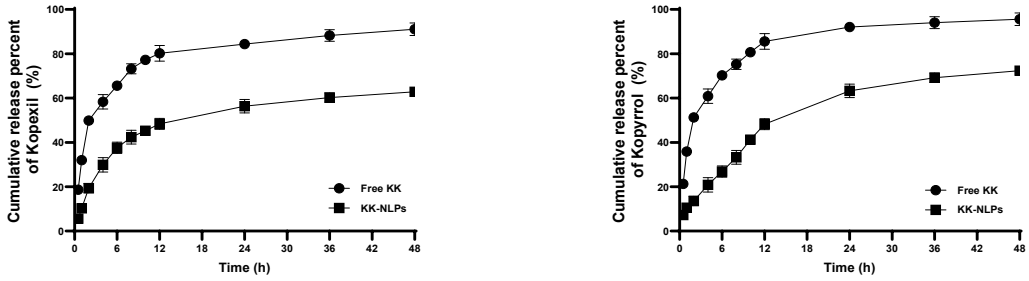

(**a**) (**b**)

Figure 3. In vitro release of kopexil (a), kopyrrol (b) from the KK-NLPs.

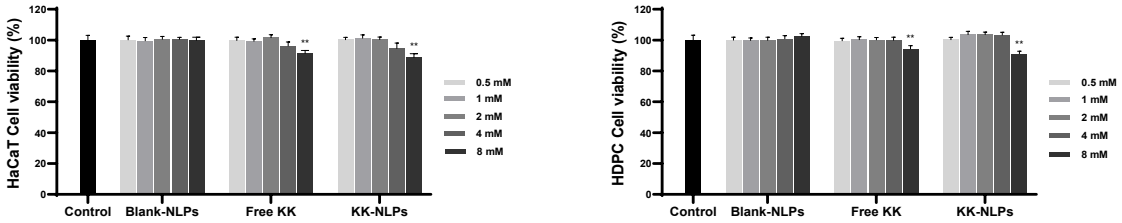

(**a**) (**b**)

Figure4. Cellular Safety Evaluation Results. Effects of Free-KK and KK-NLPs on (a) HDF, (b) HDPC. Compared with Control, $^{**}p < 0.01$.

3.4 In vivo skin permeation

In our study, clear differences were observed in the distribution of Free RhoB and RhoB-NLPs in different skin layers (Figure 5). Compared with the Free RhoB, the RhoB-NLPs penetrated deeper into the skin and were concentrated in the HFs.

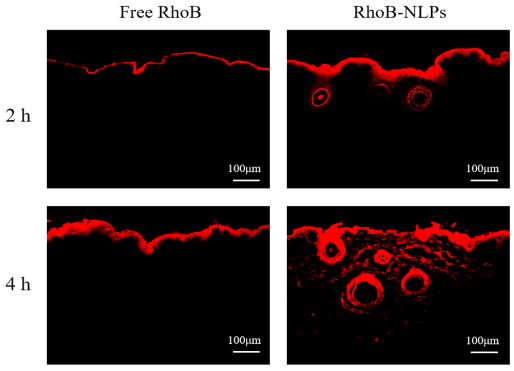

Figure5. Transdermal permeability of Free RhoB and RhoB-NLPs.

3.5. Cellular uptake

In order to verify whether the prepared NLPs could effectively deliver kopexil and kopyrrol to HDPCs, the cellular uptake of the NLPs was investigated using CLSM (Figure 6a). After 4 h incubation with Free RhoB, as a comparison, much stronger red fluorescence was observed in the cells treated with RhoB-NLPs, suggesting enhanced cellular uptake mediated by NLPs encapsulation. The relative cellular uptake for HDPCs treated with the RhoB-NLPs increased by 150.5% and 187.1% after incubation for 2 h and 4 h, respectively, in comparison with Free KK (Figure 6b).

3.6. Proliferation of HDPCs

The EdU assay results indicated that proliferating cells were significantly higher in the KK-NLPs group than in the group treated with Free KK, confirming that the KK-NLPs promoted the proliferation of HDPCs (Figure 7a and 7b).

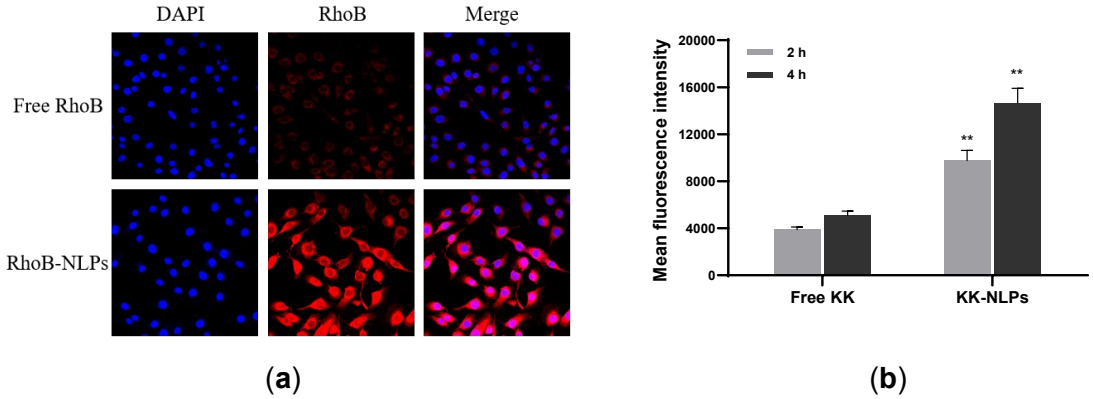

(**a**) (**b**)

Figure 6. (a) Visualization of Free RhoB and RhoB-NLPs uptake into HDPCs. (b) Relative cellular uptake of Free RhoB or RhoB-NLPs. by HDPCs. Compared with Free RhoB, $^{**}p < 0.01$.

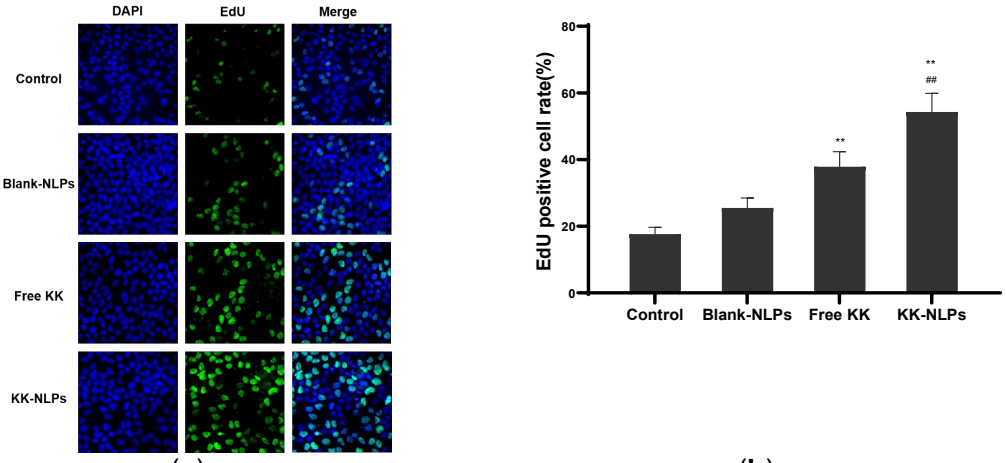

(**a**) (**b**)

Figure 7. The effect of Free KK and KK-NLPs on the proliferation of HDPCs. (a) HDPCs stained for EdU (green) and DAPI (blue). (b) Positive rate of proliferating HDPCs in EdU assay. Compared with the control, $^{**}p < 0.01$. Compared with Free KK, $^{\#\#}p < 0.01$.

3.7. Cell migration

The cell migration ability was shown in Figures 8a and 8b. After 24 h, the wound distance was significantly reduced in both the Free KK and KK-NLPs compared to the distance in the control, and the wound distance in the KK-NLPs group was significantly less than that of the Free KK group.

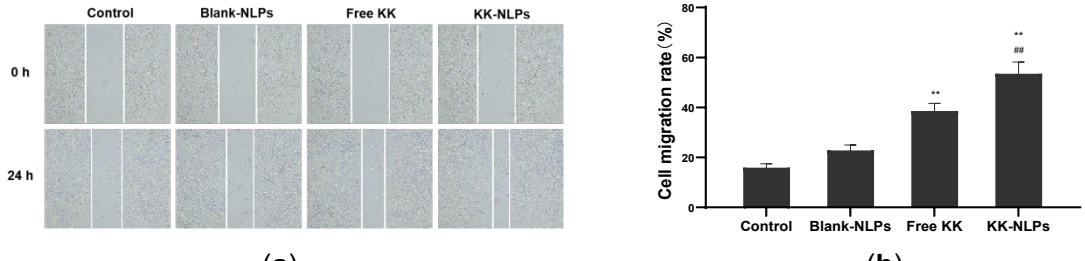

(**a**) (**b**)

Figure 8. Evaluation of the effect of Free KK and KK-NLPs on the migration of HDPCs with a scratch migration assay (A) and the cell migration rate in the corresponding experiment (B). Compared with the control, $^{**}p < 0.01$. Compared with Free KK, $^{\#\#}p < 0.01$.

3.8. Protective effect of KK-NLPs on testosterone-damaged and H_2O_2-damaged HDPCs

The anti-androgen effects of KK-NLPs on testosterone-induced HDPCs are shown in Figure 9a. Cell viability decreased dramatically to 68.7% when cells were treated with 0.1 mM testosterone, indicating that the oxidative damage cell model was successfully established. At kopexil concentrations of 100 μM and 200 μM, the cell viability of testosterone-damaged HDPCs treated with KK-NLPs was increased by 5.26% and 7.24% in contrast to the viability in the Free KK group, respectively. The above results demonstrated that loading kopexil and kopyrrol through NLPs could enhance their protective efficacy on cells damaged by testosterone.

The anti-oxidative effects of KK-NLPs on H_2O_2-induced HDPCs are shown in Figure 9b. Cell viability decreased dramatically to 48.7% when cells were treated with 1.0 mM H_2O_2, indicating that the oxidative damage cell model was successfully established. At kopexil concentrations of 50 μM and 100 μM, the cell viability of H_2O_2-damaged HDPCs treated with KK-NLPs was increased by 18.2% and 18.0% in contrast to the viability in the Free KK group, respectively.

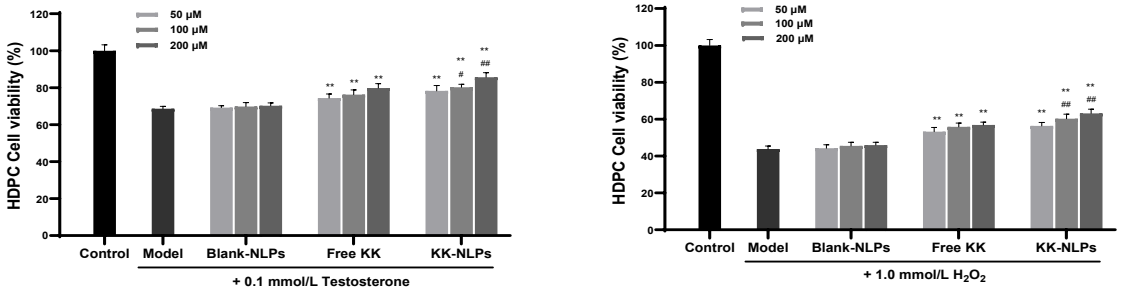

(**a**) (**b**)

Figure 9. Protective effects of Free KK and KK-NLPs against (a) testosterone-induced HDPCs and (b) H_2O_2-induced HDPCs. Compared with the control, $^{**}p < 0.01$. Compared with free KK, $^{\#\#}p < 0.01$, $^{\#}p < 0.05$.

3.10. Secretion of VEGF and bFGF

The hair growth promotion effects of KK-NLPs via analysis of the levels of VEGF and bFGF are shown in Figure 10. At a kopexil concentration of 100 μM and 200 μM, the amount of VEGF synthesized by HDPCs in the KK-NLPs group increased compared with that in the group treated with Free KK. The amount of bFGF produced by HDPCs in the group treated with KK-NLPs was higher than in the Free KK group.

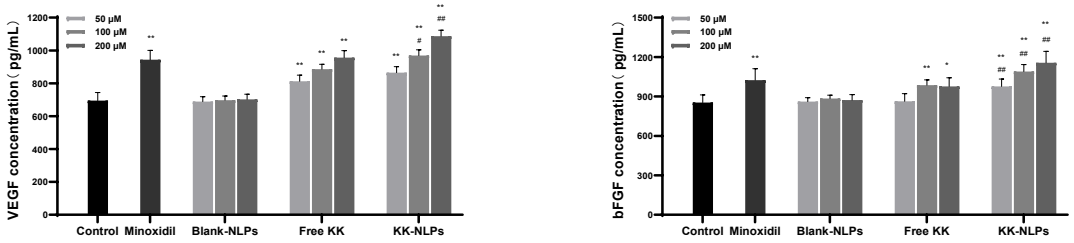

(**a**) (**b**)

Figure 10. Effects of Free KK and KK-NLPs on the secretion of (a) VEGF and (b) bFGF in HDPCs with different treatment groups. Compared with the control, $^{**}p < 0.01$, $^{*}p < 0.05$. Compared with Free KK, $^{\#\#}p < 0.01$, $^{\#}p < 0.05$.

3.11. Secretion of collagen III and EK

The effects of KK-NLPs on the secretion of collagen III by HDPCs are shown in Figure 11a. In comparison with the Free KK group, the amount of collagen III synthesized by HDPCs increased after treatment with the KK-NLPs at kopexil concentrations of 100 μM and 200 μM,

respectively. As shown in Figure 11b, the secretion of EK by HaCaT in the Free KK group was notably increased compared with the level in the control group. The amount of EK produced by HaCaT in the group treated with KK-NLPs was higher at kopexil concentrations of 200 μM compared with the levels in the Free KK group.

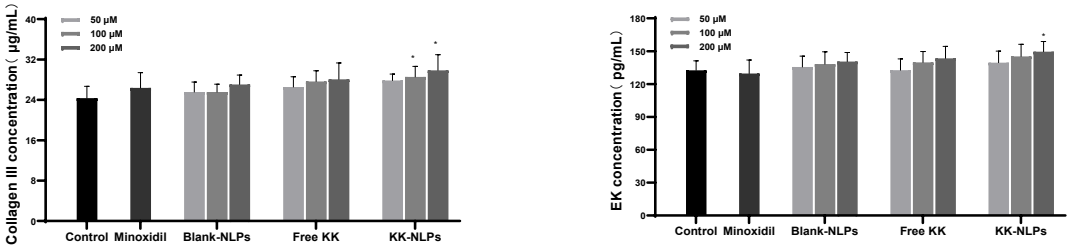

(**a**) (**b**)

Figure 11. Effects of Free KK and KK-NLPs on the secretion of Collagen III (a) in HDPCs and EK (b) in HaCaT with different treatment groups. Compared with the control, *$p < 0.05$.

3.12. Transcription of β-catenin and Cyclin D mRNA

In order to investigate the effect of KK-NLPs on the Wnt/β-catenin signaling pathway of HDPCs, the mRNA expressions of β-catenin and Cyclin D in HDPCs after co-culture with KK-NLPs. The effects of KK-NLPs on the transcription of β-catenin, Cyclin D mRNA by HDPCs are shown in Figure 12. Compared with Control, Minoxidil and KK-NLPs significantly increased the transcription levels of β-catenin and Cyclin D mRNA, while Free KK only significantly increased the transcription levels of Cyclin D mRNA. Compared with Free KK, the mRNA expression of Cyclin D by HDPCs increased after treatment with the KK-NLPs at kopexil concentrations of 200 μM.

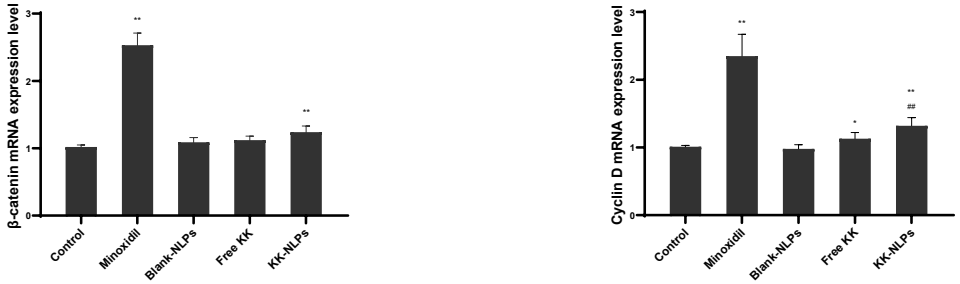

(**a**) (**b**)

Figure 12. Effects of Free KK and KK-NLPs on the transcription of β-catenin(a), Cyclin D(b), mRNA in HDPCs with different treatment groups. Compared with Control, **$p < 0.01$, *$p < 0.05$. Compared with Free KK, $^{\#\#}p < 0.01$.

4. Discussion

The majority of drugs, especially hydrophilic drugs and macromolecules, have difficulty in hair follicle penetration and retention [9]. However, NLP system is highly effective in terms of in vivo permeability and efficient delivery of the loaded active ingredients to the hair follicle [10].NLPs were uptaken by cells depending on their particle size, and the lipid component of the NLPs enhanced their affinity to the cell membranes, promoting adsorption endocytosis [11]. The NLPs prepared in this study effectively facilitated the delivery of loaded ingredients into HDPCs. Cell proliferation and migration are important properties of DPCs for HF growth and regeneration [12]. The above experimental results indicated that KK-NLPs could effectively facilitate the proliferation and migration of HDPCs.

Androgens play a major role in the pathogenesis of AGA. Oxidative stress destroys and alters a variety of molecules such as intracellular lipids, nucleic acids, and proteins, leading to apoptosis of mesenchymal stromal cells and DPCs, resulting in follicular atrophy and hair loss[13]. Increased ROS production, which can alter the structure and function of genes and proteins, leads to dysregulation of cellular behavior, causing impaired hair follicle function. KK-

NLPs can prevent ROS damage in HDPCs, and this improved ROS elimination ability may be dependent on the formulation. Loading kopexil and kopyrrol through NLPs could enhance their protective efficacy on cells damaged by androgens and oxidation.

VEGF is a biomarker of angiogenesis. It promotes hair follicle growth, and its mediated angiogenesis improves vascularity at the follicle site and increases hair growth[14]. bFGF enhances the proliferation of endothelial cells, dermal fibroblasts, and keratin-forming cells, and can enlarge hair follicles[15]. Collagen III, produced by the DP throughout the entire hair cycle, is a key component of the connective tissue in HFs and plays a critical role in maintaining the development and regulating the volume of HFs[16]. Keratin is a regulatory molecule of keratin that contributes to cell-matrix interactions, cellular infiltration, and also enhances the generation of vascular networks and the regeneration of neural networks[17]. These results demonstrated that KK-NLPs could potentiate the growth of hairs by increasing the production of VEGF, bFGF, Collagen III and EK by HDPCs.The Wnt/β-catenin signaling pathway plays a key role in the proliferation and differentiation of hair follicles and the regulation of the growth cycle[18]. β-catenin is a key protein of Wnt/β-catenin signaling pathway, and Cyclin D is one of the downstream target genes of Wnt/β-catenin signaling pathway. In our study, the mRNA expressions of β-catenin, Cyclin D increased in HDPCs after treatment with KK-NLP.

5. Conclusion

In this study, we developed, characterized and evaluated novel NLPs for transdermal co-delivery of kopexil and kopyrrol into HFs. The NLPs prepared exhibited a small and uniformly distributed particle size, high encapsulation efficiency and high co-loading capacity to various kopexil and kopyrrol. In vivo skin penetration experiments suggested that the KK-NLPs enhanced the penetration of kopexil and kopyrrol, specifically through the HF pathway. Cellular uptake studies proved that KK-NLPs could significantly improve the cellular uptake of loaded ingredients by HDPCs. Moreover, in vitro studies revealed that KK-NLPs showed synergistic effects in facilitating cell proliferation and migration, secretion of human type III collagen, VEGF, bFGF and EK, and antioxidant activity via a combinational co-delivery of kopexil and kopyrrol. KK-NLPs up-regulated the hair growth factors β-catenin, and VEGF mRNA in HDPCs. Thus, this work demonstrated the hair growth-promoting effects of KK-NLPs and provided a new strategy for the topical application of multiple kopexil and kopyrrol with NLPs for co-delivery to promote hair growth.

References

[1] Cao S, Wang Y, Wang M, et al., J Control Release. 329(2021)1-15.
[2] Inui S, Itami S. J Dermatol Sci. 61(2011)1-6.
[3] Ceruti JM, Leirós GJ, Balañá ME. Mol Cell Endocrinol. 465(2018) 122-133.
[4] Gupta AK, Talukder M, Williams G. J Dermatolog Treat. 33(2022)2946-2962.
[5] Tian L.W. , Luo D., Chen D., et al., J. Drug Deliv. Sci. Technol. 72 (2022) 103381.
[6] Phatale V, Vaiphei KK, Jha S, et al., J Control Release. 351(2022) 361-380.
[7] Zhang, S.; Zhou, H.; Chen. X. et al., ACS Appl. Mater. 16 (2024) 15701–15717.
[8] Zhou H, Shi L, Ren Y, et al., Front Cell Infect Microbiol. 22(2020)570261.
[9] Han F., Luo D., Qu W., et al., J. Drug Deliv. Sci. Technol. 57 (2020) 101693.
[10] Wei. T.,Chen. D., Mei. H., et al., Nano Life 10 (2020) 2040009.
[11] Antimisiaris SG, Marazioti A, Kannavou M, et al., Adv Drug Deliv Rev. 174(2021) 53-86.
[12] Kim BS, Na YG, Choi JH,, et al., Nanomaterials (Basel). 7(2017)241.
[13] Boisvert WA, Yu M, Choi Y, et al., BMC Complement Altern Med. 17(2017) 109.
[14] Huang PJ, Huang YC, Su MF, et al.,Photomed Laser Surg. 25(2007)183-90.
[15] Wang X, Liu B, Xu Q, et al.,Wound Repair Regen. 25(2017)270-278.
[16] Jimenez F, Alam M, Vogel JE, et al.,J Am Acad Dermatol. 85(2021) 803-814.
[17] Akanda MR, Kim HY, Park M, et al.,J Biomater Appl. 32(2017) 230-241.
[18] Rattanachitthawat N, Pinkhien T, Opanasopit P, et al., In Vivo. 33(2019)1209-1220.